Food and Bioprocess Technology (2023) 16:2692–2704
https://doi.org/10.1007/s11947-023-03097-y

RESEARCH

Hydroxyapatite-Doped Polyhydroxyethylmethacrylate Hydrogels as Smart Porous Packaging Materials

Fatma Özge Gökmen[1]

Received: 18 January 2023 / Accepted: 11 April 2023 / Published online: 24 April 2023

Abstract

The in situ radical polymerization technique has been used for synthesizing different amounts of hydroxyapatite (HAp)–doped polyhydroxyethylmethacrylate (PHEMA) films. Film-formed hydrogels were obtained, then the investigation of swelling behavior and moisture contents of composite hydrogels in aqueous solutions was carried out. The morphological and structural properties of the obtained films have been characterized by FT-IR and UV–Vis. spectrophotometer, XRD, and SEM analysis. Obtained films have shown transparent and semitransparent properties, which caused excellent UV–Vis. barrier properties. Gas transmission qualification of the films was evaluated by C, H, and N elemental analysis. HAp-doped and undoped PHEMA films were tested on cherry tomatoes as smart packaging materials. The result of the application test exhibits that these films are suitable for use as a preservative packaging of vegetables because of their visual integrity. In this way, the whole of these characterization and test results elicits the increase of shelf life of cherry tomatoes and reduction of pathogenic caused by food with HAp-doped PHEMA smart porous materials. This study presents HAp-doped PHEMA films as alternative packaging material instead of existing materials, which has a negative environmental impact.

Keywords Packaging · Hydrogel · Composite · PHEMA · Hydroxyapatite

Introduction

Packaging is the materials that extend the shelf life of the food by isolating it from the external environment and ensuring the safety of the food inside (Huang et al., 2017; Ma et al., 2020). Plastics derived from petrochemicals, such as polyethylene and polypropylene, are the most widely used packaging materials because of their light, robust, and inexpensive properties (Wu et al., 2020; Zhang et al., 2019). These petrochemical-based non-degradable plastics cause serious environmental pollution and ecological imbalance (Kameshwar & Qin, 2016). Existing plastic packaging materials cause pollution and toxicity (Gao et al., 2021). Organic compounds, initiators, catalysts, plasticizers, and solvents used to prepare plastic materials threaten human health (Huang et al., 2017). Conventional plastic materials only act as physical barriers to food contamination, which does not provide sufficient protection (Tang et al., 2016). These materials are essential for improving further food safety (Gao et al., 2021).

It takes 1000 years for petrochemical plastics to decompose in the earth's crust (Sumrin et al., 2021). Worldwide production of plastics was approximately 370 million tons in 2019. About 40% of this amount is packaging materials (Koenig-Lewis et al., 2022). Less than 30% of plastic packaging materials can be recycled (Koenig-Lewis et al., 2022). For consumers to adopt environmentally friendly, improved, and smart materials packaging, it should carefully explain that plastic waste causes harm to both human health and the environment (Dilkes-Hoffman et al., 2019; Friedrich, 2020; Koenig-Lewis et al., 2022). Production of biodegradable, bio-based food packaging materials has accelerated to replace petroleum-based chemicals (Koenig-Lewis et al., 2022).

Ensuring safe storage and food transportation is a primary responsibility today. In this context, various studies improve food packaging systems (Ozdemir & Floros, 2004; Rooney, 2005). Such studies increase food's shelf life, preserve its nutritional value, and ensure food safety (Dainelli et al., 2008). Therefore, the active packaging system is one of the food preservation features of a package. According to Appendini and Hotchkiss (2002), an active packaging system can define as the inclusion of supplements in these

✉ Fatma Özge Gökmen
fatmaozge.gokmen@bilecik.edu.tr

[1] Central Research Laboratory, Bilecik Seyh Edebali University, 11230 Bilecik, Turkey

systems to improve the performance of the packaging material (Muratore et al., 2019). In recent years, environmental pollution caused by the frequent use of petroleum-based packaging materials has become a severe problem (Piyada et al., 2013). In the last 20 years, biopolymers developed to replace petrochemical-based materials have attracted attention due to their non-toxic, biodegradable, biocompatible, and broad usage areas (El Miri et al., 2015; Shahabi-Ghahfarrokhi & Babaei-Ghazvini, 2019). Pathogenic contamination often spoils foods (Thompson et al., 1998). Food safety is essential to prevent such contamination and eliminate the threat to human and environmental health (Liu et al., 2017). In direct proportion to the increase in consumers' natural origin nutritional demands, food safety should also cover with healthier protective packaging materials (Muratore et al., 2019; Suppakul et al., 2008).

Hydrogels used for safe food packaging applications have tremendous importance in food packaging applications to control the moisture balance of products with high water content in the package due to their natural structure. Moreover, by incorporating inorganic additives into hydrogels, the antimicrobial properties of the new material can be improved. Hydrogels are three-dimensional polymeric chain networks cross-linked by physical or chemical bonds that can contain hundreds of times their masses of water (Ahmed, 2015; Chang et al., 2010). The swelling behavior of hydrogels, which have a linear or branched structure due to their ability to absorb large amounts of water, is characterized by their ability to add insoluble properties to the material due to three-dimensional network structures (Hebeish et al., 2013). Hydrogels respond to different environmental changes (stimulus) as swelling behavior in water (Argin et al., 2014). Because of all these features, it attracts great attention to creating smart food packaging systems (Chang et al., 2010). Recently, interest in the study areas has increased due to the potential of materials with water repellency properties, called "absorbent pads," to both maintain the moisture balance of food and minimize microbial contamination (Otoni et al., 2016). These new generation smart food packaging materials have various functions, such as absorption of liquids emitted from the food, modification of food and packaging contact in terms of reliability, and improved antimicrobial properties. In these functional configurations, water-absorbent hydrogels placed in food packaging are also effective in extending shelf life (Batista et al., 2019; Fernández et al., 2009). Hydrogels have a porous structure and show biodegradability and biocompatibility (Dinu et al., 2016; Dragan & Dinu, 2020). Reinforcements improve the mechanical properties of porous materials such as hydrogels (Dragan & Dinu, 2020).

Hydrogels are polymeric networks that can absorb large amounts of water (Wichterle & Lím, 1960). There is a wide range of uses that take advantage of this inflatable capacity (Caló & Khutoryanskiy, 2015). Drug delivery systems, tissue engineering, and biosensors are just a few of the application areas (Alam et al., 2018). However, poor mechanical properties are the main factor limiting the use of hydrogels in applications (Alam et al., 2018). Approaches such as composite formation, cross-linking (Oyen, 2014), and nano reinforcement addition (Alam et al., 2018) have been developed to minimize these limitations (Alam et al., 2018; Oyen, 2014). Thus, the production and design of solid hydrogels have been the focus in every field (Pereira et al., 2019).

Biodegradable polymers are of great interest due to environmental concerns and their potential in biomedical applications compared to petroleum-based ones. The number of studies on these materials, which perform better in all biological application areas, from agriculture to food packaging, from gene therapy to tissue engineering, is increasing daily (Misra et al., 2006; Nair & Laurencin, 2007). Biodegradability is one of the most fundamental properties of these materials, as this feature ensures that biodegradable polymers do not put an extra burden on today's severe environmental problems. Also, the rate of biodegradation is important for specific domains such as crystallinity, crystal modification, and molecular alignment (Li et al., 2018). 2-hydroxyethyl methacrylate (HEMA) is an important monomer due to its hydrophilic structure and active reactive feature (Li et al., 2018). Poly(2-hydroxyethyl methacrylate) (pHEMA) is a synthetic polymeric hydrogel produced by the radical in situ polymerization technique of 2-hydroxyethyl methacrylate (HEMA) monomers (Wichterle & Lim, 1960). Due to its biocompatibility, PHEMA is a Food and Drug Administration (FDA)–approved hydrogel (Montheard et al., 1992). Improvement of mechanical properties of PHEMA, like other hydrogels, eliminates many disadvantages in applications (Pereira et al., 2019). Hydroxyapatite is an inorganic bio-mineral with the chemical formula $Ca_5(PO_4)_3OH$ (HAp). Hydroxyapatite, a bio-based material, is frequently used as a base material and reinforcement material in various application areas (Pereira et al., 2019). In most of the application areas, HAp can be used in combination with other molecules and different macromolecules (Mansri et al., 2019).

This article includes the desired improved food packaging material with biodegradable polymers containing non-toxic nanomaterials. It aims to test various parameters such as antimicrobials, water swelling, pH indicators for preservation, ease of use, food preservation, and long shelf life for the obtained packaging material. Therefore, it provides alternative materials for traditional food packaging systems. In recent years, polymer-based, inorganic-doped smart composite materials have been used as smart packaging materials in many food groups from liquid foodstuffs to meat products, vegetables, and fruit groups (Abdolsattari et al., 2022; Albahr et al., 2022; Demarco et al., 2022; Duarte

et al., 2022; Emir et al., 2022; Vélez-Erazo et al., 2022). Each study to date has played a crucial role in improving the storage conditions, shelf life, nutritional value, and logistical transportation of the food chain which is most important for human health and resilient to environmental conditions. Metal oxides have been widely preferred as inorganic reinforcement materials in the studies (e.g., CuO, ZnO, AlO_x) (Abdolsattari et al., 2022; Albahr et al., 2022). Although the use of metal oxides in packaging materials has many advantages in terms of physicochemical and antibacterial properties, ionic interactions with nutrients severely limit the amount of metal oxides in composites. On the other hand, nanocomposites, which have been widely used in recent years, are also frequently used in packaging materials (Duarte et al., 2022; Luo et al., 2022; Youssef et al., 2022). Because food and human health safety studies of nanomaterials are still ongoing, these materials may encounter safety issues in mass production. Considering all these limitations, this study overcomes these limitations with the mineral HAP, which can be produced both naturally and synthetically. Furthermore, the studies can be divided into two groups: those that purchase the polymers used commercially and those that synthesize polymers from monomers. Commercially purchased and synthesized laboratory-scale products have common problems that increase the cost of raw material production when analyzed from an economic point of view. In this study, PHEMA was produced from HEMA monomer using an in situ polymerization technique with a minimum energy-saving method and with a low budget. The most common synthesis methods in the literature are compaction reactions, open ring polymerization, metal catalysts, radiation grafting polymerization, electrospinning, etc. (Abdolsattari et al., 2022; Albahr et al., 2022; Duarte et al., 2022; Liu et al., 2022; Youssef et al., 2022). The main difference of this study is that these techniques require more energy and advanced technology, as well as additional precautions during the production phase due to the toxic effects of the by-products. This work provides a highly efficient polymerization reaction using negligible amounts of cross-linkers and initiating agents, while making a big difference in providing ease of production at low temperatures, in a short time, in the desired size and quantity. Moreover, this study, with its unique synthesis packaging material and its diverse and versatile analysis methods, fills knowledge gaps that the existing literature fails to fill.

Experimental

Materials and Methods

The films obtained for use as a smart packaging material with a different amount (0.05%wt, 0.1%wt, and 0.5%wt) of HAp (hydroxyapatite) (supplied from Aldrich Chemistry) additive during the polymerization of HEMA. HAp was an inorganic reinforcement chemical. Along with the study, deionized water was used in all experimental setups. While synthesis of the PHEMA (poly(2-hydroxyethyl methacrylate) hydrogels, HEMA (hydroxyethylmethacrylate) (supplied from Aldrich, 97%) was used as a monomer (2.5 M), APS (ammonium persulfate) (supplied from Sigma-Aldrich, ≥ 98.0%) was used as an initiator (0.005 M), NNMBAAm (N, N –methylene bis(acrylamide)) (supplied from Sigma-Aldrich, 99%) was used as a cross-linker (0.05 M), and TEMED (N, N, N′, N′-Tetramethylethylenediamine) (supplied from Sigma, Life Science, ≥ 99%) was used as a catalyst. In situ radical polymerization technique was enforced to obtain HAp-doped and undoped PHEMA films.

Preparation of HAp-Doped PHEMA Films

PHEMA hydrogels were synthesized by the in situ radical polymerization technique. The concentrations of the reactants were optimized, such as 2.5 M monomer, 0.005 M initiator, and 0.05 M cross-linker. HAp as an additive was poured into the polymer solution (0.05%wt., 0.1%wt., and 0.5%wt.) at 50 °C, 16 h. Solutions were poured into the glass Petri dishes (60 × 15 mm) by equal volume (15 mL). Then, films were kept at 40 °C overnight. A schematic illustration of intermolecular attractions between PHEMA and HAp is given in Fig. 1. As seen in Fig. 1, Ca^{2+} ions attack -OH groups of PHEMA in the presence of a radical initiator. Sample identification is reported in Table 1.

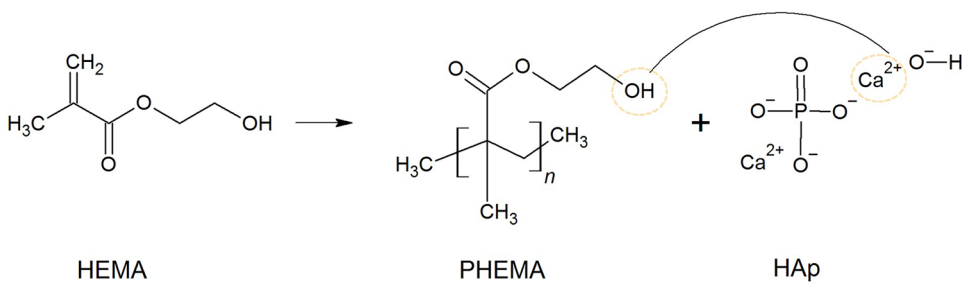

Fig. 1 A schematic illustration of mechanism between PHEMA and HAp

Characterization of HAp-Doped PHEMA Films

Fourier transform infrared (FT-IR) spectra of the HAp-doped and undoped PVA films were evaluated by Perkin Elmer, Spectrum 100 in the attenuated total reflection (ATR) mode between 400 and 4000 cm^{-1} with a 4 cm^{-1} resolution. X-ray diffraction (XRD) patterns of the composite films were acquired in a Panalytical Empyrean diffractometer with Cu*K*a radiation of 45 kV, 40 mA, and a scanning range between 10 and 60°. Field emission scanning electron microscopy (FESEM) images of the films' surfaces were obtained by Carl Zeiss, Supra 40VP microscope, with the samples sputter-coated previously under vacuum with platinum, and applied 10 kV of acceleration voltage. Quantification of elements was achieved by electron dispersive X-ray spectroscopy (EDX). Gas transmission properties of the films were evaluated by LECO, a CHNS-628 elemental analysis device. Carbon, hydrogen, and nitrogen contents of HAp-doped and undoped PHEMA films were tested by burning in the furnace at 950 °C. UV–Vis. measurements were measured between 200 and 700 nm to determine the light barrier properties (Jayakumar et al., 2019). All films were cut into rectangular pieces and placed in a UV–Vis. spectrophotometer (Perkin Elmer, Lambda 25).

Swelling Behavior of HAp-Doped PHEMA Films

The swelling behavior of obtained hydrogels was examined in aqueous solutions, and the swelling response of the samples was recorded. Gel conversion (GC %), cross-linked (CL %), and swelling (S %) values of the samples were calculated by Eqs. (1), (2), and (3), respectively (Gokmen et al., 2021). m_0 is defined total amounts of monomer, cross-linker, and initiator; m_1 is the weight of the hydrogels; m_1' is the weight of the dried hydrogel, and m_2 is the weight of the hydrogel after being washed twice the time; m_t is the weight of the swollen hydrogel at t time, and m_i is the dry weight at time zero.

$$GC(\%) = \frac{m_1}{m_0} \times 100 \tag{1}$$

Table 1 Sample identification

Sample name	Reactants				
	HEMA	Initiator	Cross-linker	Catalyst	HAp
HJ	2.5 M	0.005 M	0.05 M	**20 µL**	**-**
HJ-2	2.5 M	0.005 M	0.05 M	**20 µL**	**0.0025 g**
HJ-3	2.5 M	0.005 M	0.05 M	**20 µL**	**0.005 g**
HJ-4	2.5 M	0.005 M	0.05 M	**20 µL**	**0.025 g**

$$CL(\%) = \frac{m_2}{m_1'} x 100 \tag{2}$$

$$S(\%) = \frac{m_t - m_i}{m_i} \times 100 \tag{3}$$

One essential property of hydrogels is swelling behavior in liquids (Dragan & Dinu, 2020). The pore structure of hydrogels quickly removes solvent molecules from the environment during swelling (Dragan & Dinu, 2020). Calculations of water content at equilibrium (EWC, Eq. (4)) and water vapor transmission rate (WVTR, Eq. (5)) were used to explain the swelling behavior of hydrogels (Dragan & Dinu, 2020).

$$EWC = \frac{W_e - W_d}{W_e} \times 100 \tag{4}$$

$$WVTR = \frac{W_i - W_f}{At} \times 100 \tag{5}$$

W_t and W_d represent the weights of the hydrogel in the swollen state at time t and in the dried state, respectively. W_e is the weight of the swollen hydrogel at equilibrium. W_i is the weight of the swollen hydrogel and W_f is the weight of the swollen hydrogel measured after 24 h outside the solvent. At Eq. (5), t is the 24 h and A is the area of the piece of hydrogels in the m^2 unit (Dragan & Dinu, 2020).

The moisture content (MC) of the films cut into 2 × 2 cm^2 dimensions was calculated by Eq. (6) (Haghighi et al., 2021). Each sample was constant weighted at 105 ± 2 °C. In Eq. (6), M_0 presents the weight of the hydrogel at room temperature, and M is the weight of the hydrogel which was constantly weighted.

$$MC(\%) = \frac{M_0 - M}{M_0} \times 100 \tag{6}$$

Food Packaging Application

To investigate the packaging activity, cherry tomatoes were covered by HAp-doped and undoped PHEMA films and tracked for 21 days. As a control sample, uncovered tomatoes were placed into Petri dishes and followed under the same conditions. It is crucial to select undamaged tomatoes covered by washed films for the application test. Shrinkage of the control sample and coated samples was tracked and photographed at room temperature. The fresh keeping effect of HAp-doped films was determined by measuring the weight loss rate of cherry tomatoes (Eq. (7)).

$$W_{loss}(\%) = \frac{W_0 - W_L}{W_0} \times 100 \tag{7}$$

where W_0 and W_L were the weighted of cherry tomatoes before packaging and after packaging, respectively.

Results and Discussion

FT-IR

The polymerization was first evaluated by ATR-FT-IR spectroscopy. The absence of absorption bands of the methacrylate group of the HEMA monomer at 829 cm^{-1} and 1648 cm^{-1}, which is attributed to CH out-of-plane and C–C stretch vibrations, respectively, confirms that vinyl carbon groups are formed as a result of the polymerization (Castro et al., 2019). The presence of a band of stretching vibration at 1709 cm^{-1} is attributed to the presence of C = O groups belonging to PHEMA (Wang et al., 2022; Yavuz et al., 2016). In another study, C = O stretching vibrations of PHEMA and HEMA were observed at 1728 cm^{-1} and 1719 cm^{-1}, respectively (Wang et al., 2023). It can be said that in the presence of radical initiator, the C = O band of the cross-linked films shifts to 1709 cm^{-1}. In Fig. 2, FT-IR spectra of PHEMA biofilms containing different amounts of HAp are given. The black line belongs to plain PHEMA. FT-IR spectra of nanocomposite hydrogels encoded with HJ-2 (0.05%wt.), HJ-3 (0.1%wt.), and HJ-4 (0.5%wt.) are shown with red, blue, and green lines, respectively. The bands belonging to the phosphate group confirming the formation of HAp in film samples were obtained in the 1100 cm^{-1} and 575 cm^{-1} range as seen in previous studies (Mahroug et al., 2019; Mansri et al., 2019). The corresponding FT-IR spectra of HAp were obtained in agreement with previous results in the literature (Chaudhuri et al., 2016; Hui et al., 2015). O–P–O bending modes were seen at 552 cm^{-1} and 665 cm^{-1} regions in HJ-2 and HJ-4. The 2475 cm^{-1} (green line) band was assigned to the P-O–H stretching mode and the 1451 cm^{-1} band was assigned to the P–O–H in-plane bending mode. Other films, except HJ-4 in Fig. 2, were found to have a similar IR spectrum. This indicates that the surfaces have the same functional groups. Also, in HJ-2 spectrum, a small amount of HAp was observed in the bands; but in HJ-3, there are no peaks of HAp could be observed in the spectrum due to the limitations arising from the choice of the area where the analysis was performed. Surface functional group diversity was revealed in HJ-4, where the increasing amounts of HAp were the highest (0.5%wt.). Also, according to the literature, the peak at 569 cm^{-1} is due to the PO_4^{3-} bending modes of the apatite structure (Mary et al., 2016). These bands of HAp are also compatible with the XRD results of the samples.

XRD

In Fig. 3, the XRD pattern of the HAp-doped and undoped PHEMA films is given. Accordingly, in the XRD spectrum of the PHEMA film with the highest HAp content (HJ-4), peaks compatible with Reference code: ICDD data 98–015-1414, Apatite, hexagonal structure was observed. It is seen from the spectrum that the amorphous XRD peaks of PHEMA decrease with the addition of HAp (Koçyiğit et al., 2013). On the other hand, as the amount of HAp in the films increased, the crystal peaks of HAp in the spectrum increased. A composite film with the highest HAp concentration (0.5% by weight) (HJ-4) exhibited the maximum number of HAp peaks in Fig. 3. This was explained in previous studies because at high HAp concentration, the grains are highly oriented, and thus the crystallinity of the

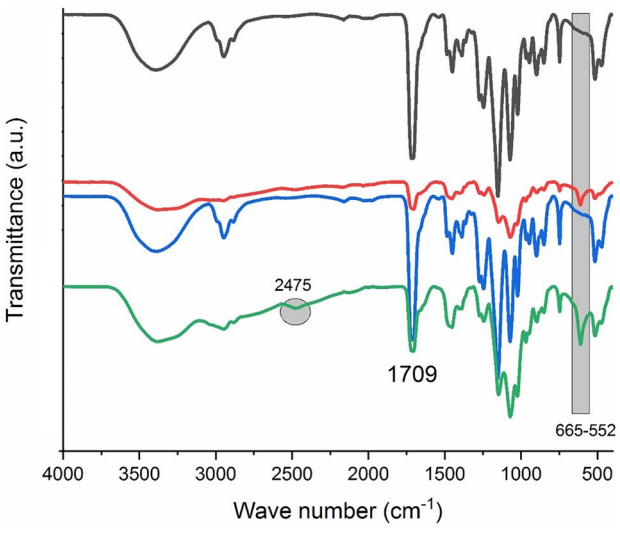

Fig. 2 FT-IR spectrum of HAp-doped and undoped PHEMA films (black line: HJ; red line: HJ-2; blue line: HJ-3; and green line: HJ-4)

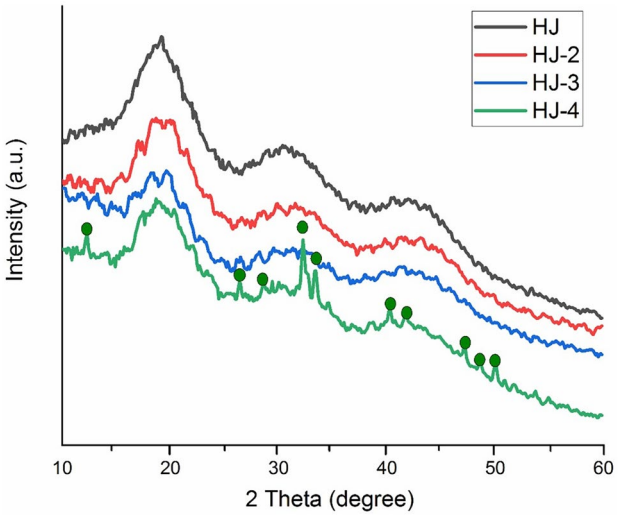

Fig. 3 XRD pattern of HAp-doped and undoped PHEMA hydrogels

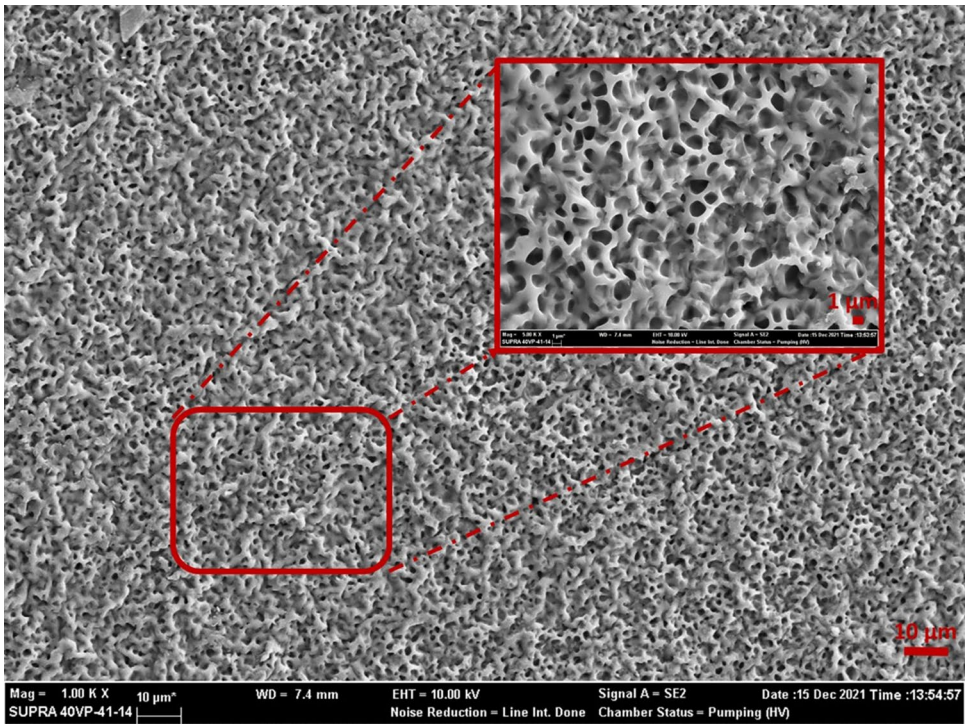

Fig. 4 The picture in picture of undoped PHEMA hydrogel at 1000 × and 5000 × magnifications

composite is improved as observed from the XRD peaks (Chaudhuri et al., 2016).

SEM–EDX

In Fig. 4, the morphological image of plain PHEMA hydrogel without HAp additive is given in two different magnifications in the picture of picture. While it was seen how homogeneous the surface was at 1000 × magnification, the microporous structure of PHEMA was observed at 5000 × magnification.

SEM images of HAp-doped PHEMA films are given in Fig. 5. Accordingly, HAp is mostly homogeneously dispersed on the polymer matrix. When the film surfaces were examined at each magnification by SEM analyses, no particles were found inside or at the edges of the pores. Due to this observation, it is stated that the HAp distribution on the film surfaces is homogeneous. However, agglomeration occurred on the surface of the composite films at the highest concentration (HJ-4). HAp also showed an effect on the porosity of the films (Temel et al., 2020). Compared to the plain PHEMA film surface, the surface porosity decreased at all other three concentrations (HJ-2, HJ-3, and HJ-4). However, while it is expected that the swelling behavior will decrease in direct proportion to the shrinkage of the pores, contrary to expectations, the swelling rates of the films increased when the amount of HAp increased due to the water-holding ability of HAp.

The semi-quantitative EDX results of PHEMA films prepared in this study, doped and undoped with different amounts of HAp, are given in Table 2. It was confirmed that HAp addition increased when looking at the atomic Ca and P amounts on the plain PHEMA surface. Although HJ-2 and HJ-3 were similar due to their low HAp amounts, atomic Ca and P values were found 0.53% and 0.81%at., respectively, in HJ-4.

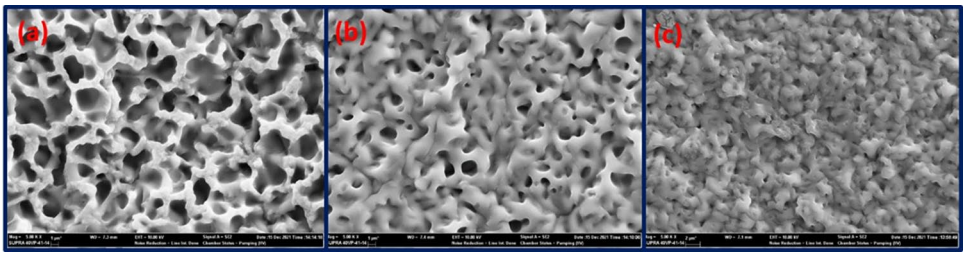

Fig. 5 HAp-doped PHEMA hydrogels **a** HJ-2 (0.05%wt.), **b** HJ-3 (0.1%wt.), and **c** HJ-4 (0.5%wt.)

Table 2 EDX analysis of samples

Samples	Elements (%at.)			
	C	O	Ca	P
HJ	**67.21**	**32.79**	**-**	**-**
HJ-2	**66.77**	**32.82**	**0.01**	**0.41**
HJ-3	**66.11**	**33.43**	**0.01**	**0.46**
HJ-4	**65.86**	**32.80**	**0.53**	**0.81**

Gas Transmission

Obtained films' gas transmission properties were investigated under N_2, air, and smoke (CO_x) for 5 min, separately. The samples were humidified before gas exposure. Carbon, hydrogen, and nitrogen contents of HAp-doped and undoped PHEMA films which have known initial weight were measured by burnt in the furnace at 950 °C. The oxygen content of the samples was calculated by completing the total C, H, and N elements up to 100. C, H, N, and O contents of HAp-doped and undoped PHEMA biofilms are given in Fig. 6. According to the results, the carbon and oxygen amounts of plain PHEMA and HAp-doped PHEMA films, which were not exposed to any gas, were almost the same (~ 50%wt. carbon and ~ 40%wt. oxygen).

On the other hand, N_2, air, and CO_x gas exposures showed an increase in the amount of oxygen compared to the initial values. When N_2 was passed through the films, the film with the highest oxygen content (70%wt.) was the HJ-4-coded film (marked with a "star shape" in the bar indicated by HJ-4-N_2). As expected in the behavior of films exposed to air, HJ-4 with the highest amount of HAp contains 63% O_2, while HJ contains 72% O_2. While the amount of HAp shrinks the PHEMA pores on the film surfaces, it retains a large amount of O_2 due to the chemical structure of HAp. Also in plain PHEMA, which is coded with HJ-air and marked with a "triangle," the large pore structure shows the barrier property in gas transmission. Similar results were observed with CO_x (smoke) exposure. The high amount of O_2 obtained in each gas exposure can be interpreted by the fact that the Ca and PO_4^{3-} groups of HAp retain a high amount of water vapor, NO_x, and CO_x gases. The gas permeability results of these films, developed for use in food packaging, significantly reduce the transmission of oxygen and water vapors, two unfavorable gases in the packaging (Nguyen et al., 2021). These properties showed that the produced films are suitable for packaging materials.

UV-Light Transmission

The UV barrier property of packaging materials is an important parameter that should examine to reduce lipid oxidation in foods, prevent loss of nutritional value, eliminate color and taste deterioration, and extend food shelf life (Haghighi et al., 2020). UV–Vis. transmissions of HAp-doped and undoped PHEMA films are given in Fig. 7 in the range of 200–700 nm. According to the results, the UV-light transmission of the films decreased as the amount of HAp increased. In the wavelength range of 200–700 nm, plain PHEMA (HJ coded) used as the control sample showed the highest UV-light transmission property. As seen in Fig. 7, each film's visible light transmission is higher than the UV transmission.

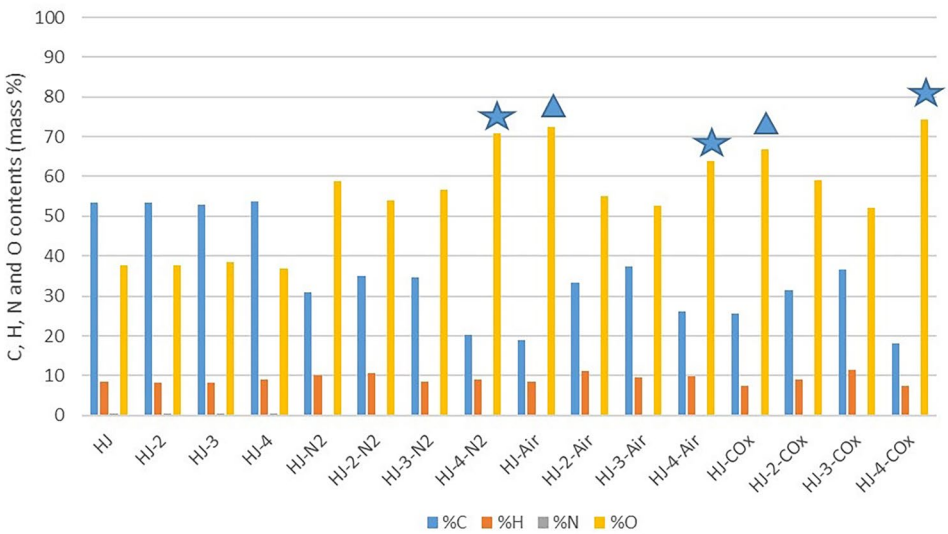

Fig. 6 C, H, N, and O contents of HAp-doped and undoped PHEMA biofilms

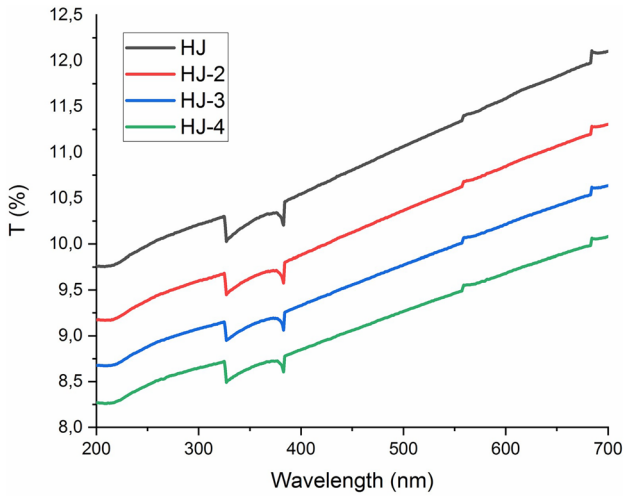

Fig. 7 UV–Vis. transmissions of HAp-doped and undoped PHEMA films

Swelling Behaviors of the HAP-Doped/Undoped PHEMA Films

To determine the swelling behavior of the films in water, the films were cut into 1×1 cm^2 pieces. The weights of the first dry state were measured and recorded (m_0). Each piece of film was placed in 5 mL of distilled water to examine its swelling properties. After wiping the excess water on the films with filter paper for different time intervals until the 50th h, the weights of the swollen state were taken and recorded (m_t). The GC %, CL %, EWC, WVTR, and MC % values of the films were calculated using Eqs. (1), (2), (4), (5), and (6) and are given in Table 3. According to these results, the films achieved polymerization and cross-linking with 100% conversion. For plain PHEMA, the conversion is 93%. The reason for this can be given as the error in the weighing taken after polymerization (Temel et al., 2019a, b). According to Table 3, the films' equilibrium water content (EWC) was calculated as approximately 61% for plain HEMA and 64%, 63%, and 63% for HAp-doped PHEMA films, respectively. The amount of EWC increased as HAp was added to the PHEMA films. The highest EWC value is seen in HJ-2 because HAp is homogeneously distributed on the film surface without agglomerate. The interpretation of the homogeneity of HAp particle distributions was based on SEM images. The water content of hydrogels at equilibrium appears to be increased in HAp-doped hydrogels compared to non-doped hydrogels. HAp-doped PHEMA films are more hydrophilic than plain PHEMA films. Therefore, the presence of HAp in the composite caused an increase in the EWC value. As the amount of HAp in the content increased, the hydrogel networks became more hydrophilic and absorbed more water (Yang et al., 2016). Although the amounts of HAp in HJ-3 and HJ-4 are quite different, the similar EWC values in both hydrogels mean that the intermolecular interaction of HAp molecules in the films with PHEMA is strong at increasing HAp amounts. Looking at the WVTR values of the films, as the HAp amount increases, the WVTR of the films slightly reduces from ~ 344,000 to 254,000 g.day^{-1}.m^{-2}. Reducing WVTR is vital in increasing the shelf life of packaged foodstuffs (Haghighi et al., 2021). The moisture content (MC) of the films is presented in Table 3. The MC values ranged from 4.5 to 6%. Moisture content was calculated according to Eq. (6). After the films were taken out of the oven, they were kept in a desiccator for 30 min to avoid sudden moisture and then weighed; for each film, triplicates were tested. According to these results, the moisture content of the plain PHEMA hydrogel is 6.19%. As the amount of HAp increased, the % moisture content of the films decreased. Also, the amount of free water vapor decreased (Jayakumar et al., 2019). HAp-doped PHEMA films, which show more swelling behavior than undoped PHEMA films, shrink when dried at 105 °C. The moisture content of the shrinking composite films is less. HAp-doped PHEMA intermolecular interactions have the ability to retain more water when the films swell in water, and contain less moisture in the shrinkage behavior. As a result, the interaction between the polymer-inorganic reinforcing material is stronger than the polymer–polymer interaction.

Table 3 The GC %, CL %, EWC, WVTR, and MC % values of the films

	CL (%)	GC (%)	EWC (%)	WVTR (g.day^{-1}.m^{-2})	MC (%)
HJ	100.29	92.99	61.19	343,888.9	6.19
HJ-2	100.04	107.05	64.03	329,777.8	5.75
HJ-3	100.03	104.75	63.32	315,041.3	5.85
HJ-4	100.13	104.26	63.47	254,133.3	4.47

% Swelling values were calculated according to Eq. (3) and are given in Fig. 8. According to Fig. 8, each film reached a swollen equilibrium state after 24 h. In addition, swelling values increased as the HAp content in the films increased. The reason for this is the water-holding ability of Ca/P ratios in the amount of HAp. In agreement with the literature, the addition of HAp improved the hydrophilicity of the films (Chaudhuri et al., 2016). As can be seen from the figure, the swelling of the films in water occurred rapidly and the equilibrium water uptake was reached after 24 h. Compared to PHEMA (160%), the water swelling rate of HAp-doped PHEMA films increased significantly (about 180%). The addition of HAp to the hydrogel network may have contributed to this result by introducing more hydrophilic functional groups (-OH) (Bayramoğlu et al., 2002).

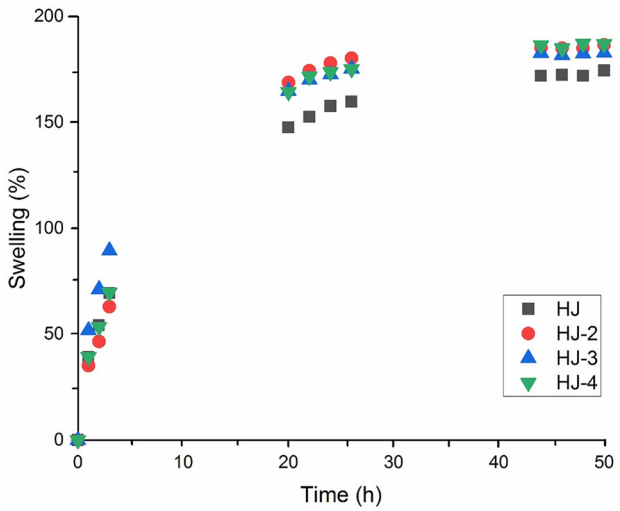

Fig. 8 % Swelling values of the HAp-doped and undoped PHEMA films

Although the swelling values for HJ-2, HJ-3, and HJ-4, which reached equilibrium in Fig. 8, are close to each other, the swelling rates of the hydrogels are not the same from the beginning. According to this result, films with higher HAp content swelled faster as expected. When the films reached equilibrium, depending on the amount of HAp, the films rapidly reached saturation and did not swell at a higher rate.

Food Packaging Application

It is crucial to demonstrate the application of HAp-doped and undoped PHEMA films in food packaging (Min et al., 2020). Cherry tomatoes, which can easily deform due to their shelf life and sensitive outer skin, were selected for the application test in this study. HAp-doped and undoped PHEMA biofilms application for cherry tomatoes packaging was tested at room temperature (25 °C) for 21 days. The experiment was divided into five groups: the control group (coded by Control) and the HAp-doped and undoped PHEMA biofilms coded HJ, HJ-2, HJ-3, and HJ-4. The degree of decay of cherry tomatoes was recorded by photographing (Min et al., 2020). Photos of cherry tomatoes packaged by HAp-doped and undoped PHEMA biofilms and unpackaged tomato samples are given in Fig. 9. Figure 9 shows the changes in the cell wall morphology of cherry tomatoes over time. Figure 9 shows that fresh tomatoes are full of moisture on day zero. In Fig. 9, samples covered with HAp-doped and undoped PHEMA film are given in

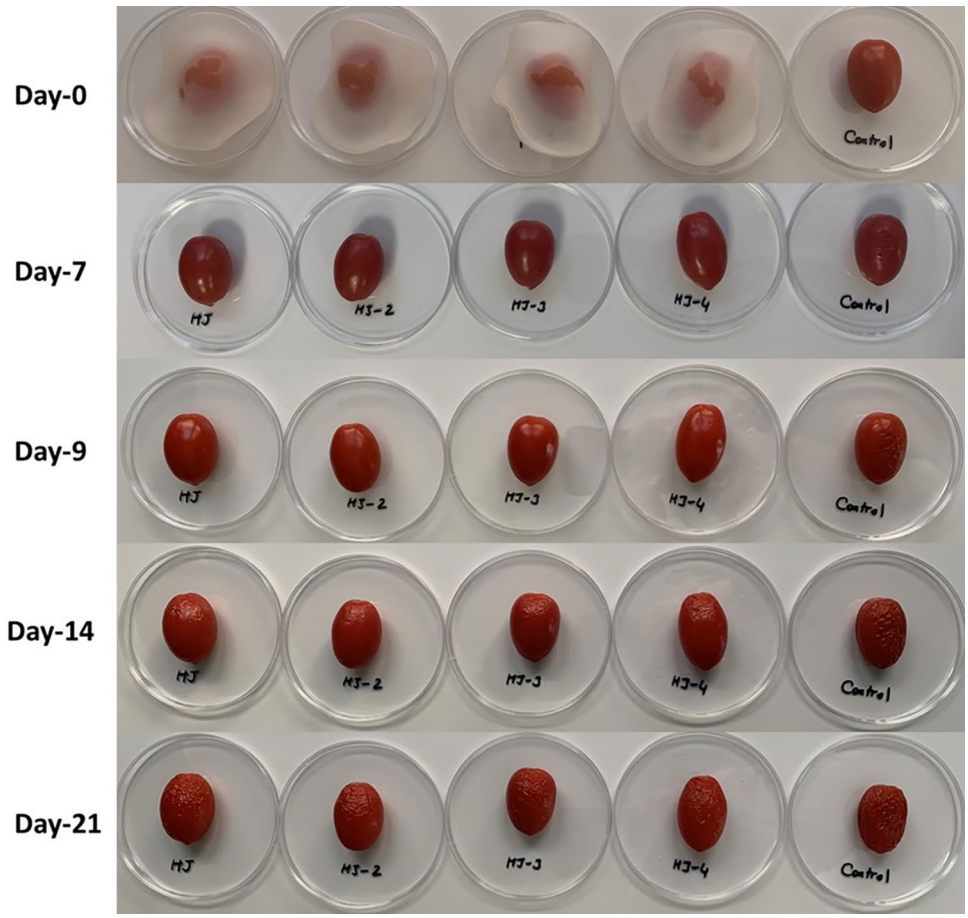

Fig. 9 Cherry tomatoes were photographed after storage for 21 days. Left to the right; plain PHEMA (HJ), 0.05%wt. HAp-doped PHEMA (HJ-2), 0.1%wt. HAp-doped PHEMA (HJ-3), 0.5%wt. HAp-doped PHEMA (HJ-4) composite coatings

the image of day zero. In later photo shoots, the films were temporarily removed. On the 7th day, the unpackaged tomato started to shrivel, which can be seen from the changes in its morphology. On the 14th day, film-coated cherry tomatoes started to shrivel. In the following days, the surfaces of the tomatoes became slightly dry and wrinkled. At the end of the 21st days, all the tomatoes have almost completely lost their moisture and shriveled. The results showed that the films effectively extended the shelf life of tomatoes.

Weight loss of fruit and vegetables is related to the evaporation of water in their structure (Min et al., 2020). Rapid water loss is one of the most critical factors that cause food to shrink and rot (Min et al., 2020). Due to the low mechanical strength of cherry tomatoes, it is a sensitive food type with a short shelf life and fast shrinkage. Weight loss of the films was calculated by Eq. (7). As seen in Fig. 10, cherry tomatoes' cell respiration and water evaporation rate are most significant under unpackaged conditions. Therefore, the highest weight loss was observed in the control sample. However, weight loss was reduced when tomatoes were packaged with PHEMA films. HAp-doped PHEMA films for packaged applications on cherry tomatoes delay evaporation and water loss. The % weight loss of unpackaged tomatoes (control sample) is the highest among the films, with 33%. The weight loss of plain PHEMA-coated tomato (HJ) after 21 h is 23%. The moisture retention properties of HAp due to Ca^{2+} and PO_4^{3-} ions caused the tomatoes to remain without shrinkage for extended periods. Thus, tomatoes retain moisture in their structures longer. It extends their shelf life. In addition, as seen in Fig. 10, the weight loss of the control sample occurs rapidly from the 1st day, while the weight loss of packaged tomatoes takes more time. The best moisture-holding ability was achieved in the HJ-2-coded film (18%), in which HAp was homogeneously distributed. The expected result was obtained in tomatoes packaged with HJ-2. HAp in the polymer matrix is responsible for moisture retention in cherry tomatoes. The best result was obtained in the film where the polymer-inorganic material interaction was the best, not as the amount of HAp increased. According to Fig. 10, intermolecular interactions are stronger than intramolecular interactions in HJ-2. In HJ-3, intramolecular interactions are higher than intermolecular interactions. In HJ-4, which has the highest amount of HAp, the interaction between HAp molecules is more than polymer–polymer interaction. The excess amount of HAp caused HJ-4 to be a better moisture barrier than HJ-3.

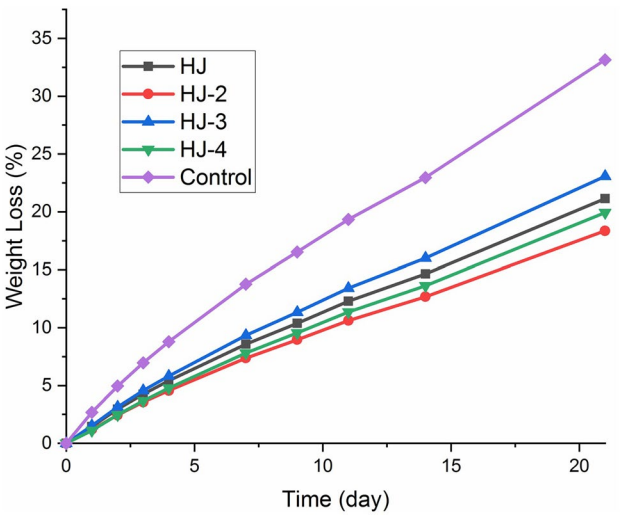

Fig. 10 Weight loss of the plain PHEMA, HAp-doped PHEMA, and control films

Conclusion

Active and smart packaging, protection of food from the external environment, and good transportation are the most critical features desired. With technological innovations, studies are constantly improving, and this development provides safe packaging and longer shelf life to foods. This study provides information on using HAp-doped and undoped PHEMA biofilms as smart packaging materials. The investigated parameters, water barrier properties, UV barrier properties, gas transmission properties, application field tests, and structural and morphological characterizations were discussed. The obtained films were transparent, flexible, and exhibited good mechanical properties. The films produced as packaging materials were obtained in good appearance and homogeneous thickness. The findings of the elastic physical behavior of the films were visually monitored instead of mechanical properties. These values will be presented quantitatively in complementary studies where stress–strain tests and biodegradable behavior will be examined. The same can be said for homogeneous thickness. Structural characterization results showed good compatibility between various HAp amounts and polymer. On the other hand, as HAp addition increased, the amount of heterogeneous phase in the films also increased. Thus, ensuring the homogeneous distribution of HAp in the films was the most critical challenge in this study. According to the XRD analysis results, the matrix crystallinity was significantly affected by the presence of HAp particles. The morphologies of the films were examined by SEM analysis. Accordingly, the micro- and mesoporous structure of the films is the most important structural feature affecting the results in gas transmission, swelling behavior, and weight loss tests. The advantage it brings, apart from using the films obtained in food packaging, also allows development. It opens up new opportunities for new material conversions. Considering their swelling behavior, adding HAp to the PHEMA matrix improved the hydrophilicity of the films. The films obtained

in this study can keep the environment dry by absorbing the resulting moisture from the tests performed on cherry tomatoes, thus preventing the rapid deterioration of foods. The data obtained from the study results showed that such films could be an alternative to traditional method packaging materials. This study focused on physicochemical and analytical characterizations. Commercialization efforts will be accelerated with biological activity tests, mechanical strength tests, and market research planned to be carried out in the follow-up study. Commercial availability of HAp-doped PHEMA composite biofilms will result in future market research. Currently, the results of this study show that it is a promising packaging material that can meet the market's needs with food safety and increased shelf life.

Acknowledgements The author thanks the Bilecik Seyh Edebali University, Central Research Laboratory for the characterizations of this study.

Author Contribution Fatma Özge Gökmen designed the study and the experimental setups. Fatma Özge Gökmen evaluated the characterization results and prepared all figures and tables in the manuscript. Fatma Özge Gökmen was the only one responsible for writing, editing, and reviewing the manuscript.

Data Availability All data generated or analyzed during this study are included in this published article.

Declarations

Conflict of Interest The author declares no competing interests.

References

Abdolsattari, P., Rezazadeh-Bari, M., & Pirsa, S. (2022). Smart film based on polylactic acid, modified with polyaniline/ZnO/CuO: Investigation of physicochemical properties and its use of intelligent packaging of orange juice. *Food and Bioprocess Technology, 15*(12), 2803–2825. https://doi.org/10.1007/s11947-022-02911-3

Ahmed, E. M. (2015). Hydrogel: Preparation, characterization, and applications: A review. *Journal of Advanced Research, 6*(2), 105–121. https://doi.org/10.1016/j.jare.2013.07.006

Alam, A., Zhang, Y., Kuan, H. C., Lee, S. H., & Ma, J. (2018). Polymer composite hydrogels containing carbon nanomaterials—morphology and mechanical and functional performance. *Progress in Polymer Science, 77*, 1–18. https://doi.org/10.1016/J.PROGPOLYMSCI.2017.09.001

Albahr, Z., Al-Ghamdi, S., Tang, J., & Sablani, S. S. (2022). Pressure-assisted thermal sterilization and storage stability of avocado puree in high barrier polymeric packaging. *Food and Bioprocess Technology, 15*(11), 2616–2628. https://doi.org/10.1007/s11947-022-02904-2

Appendini, P., & Hotchkiss, J. H. (2002). Review of antimicrobial food packaging. *Innovative Food Science & Emerging Technologies, 3*(2), 113–126. https://doi.org/10.1016/S1466-8564(02)00012-7

Argin, S., Kofinas, P., & Lo, Y. M. (2014). The cell release kinetics and the swelling behavior of physically crosslinked xanthan–chitosan hydrogels in simulated gastrointestinal conditions. *Food Hydrocolloids, 40*, 138–144. https://doi.org/10.1016/J.FOODHYD.2014.02.018

Batista, R. A., Judith, P., Espitia, P., Souza, J. D., Quintans, S., Machado, M., et al. (2019). Hydrogel as an alternative structure for food packaging systems. *Carbohydrate Polymers, 205*, 106–116. https://doi.org/10.1016/j.carbpol.2018.10.006

Bayramoğlu, G., Kaya, B., & Arica, M. Y. (2002). Procion brown mx-5br attached and lewis metals ion-immobilized poly(hydroxyethyl methacrylate)/chitosan ipns membranes: Their lysozyme adsorption equilibria and kinetics characterization. *Chemical Engineering Science, 57*(13), 2323–2334. https://doi.org/10.1016/S0009-2509(02)00141-0

Caló, E., & Khutoryanskiy, V. V. (2015). Biomedical applications of hydrogels: A review of patents and commercial products. *European Polymer Journal, 65*, 252–267. https://doi.org/10.1016/J.EURPOLYMJ.2014.11.024

Castro, K. A. D. F., Moura, N. M. M., Simões, M. M. Q., Cavaleiro, J. A. S., Faustino, A. F., Cunha, Â., et al. (2019). Synthesis and characterization of photoactive porphyrin and poly (2-hydroxyethyl methacrylate) based materials with bactericidal properties. *Applied Materials Today, 16*, 332–341. https://doi.org/10.1016/j.apmt.2019.06.010

Chang, C., Duan, B., Cai, J., & Zhang, L. (2010). Superabsorbent hydrogels based on cellulose for smart swelling and controllable delivery. *European Polymer Journal, 46*(1), 92–100. https://doi.org/10.1016/J.EURPOLYMJ.2009.04.033

Chaudhuri, B., Mondal, B., Ray, S. K., & Sarkar, S. C. (2016). A novel biocompatible conducting polyvinyl alcohol (PVA)-polyvinylpyrrolidone (PVP)-hydroxyapatite (HAP) composite scaffolds for probable biological application. *Colloids and Surfaces B: Biointerfaces, 143*, 71–80. https://doi.org/10.1016/j.colsurfb.2016.03.027

Dainelli, D., Gontard, N., Spyropoulos, D., Zondervan-van den Beuken, E., & Tobback, P. (2008). Active and intelligent food packaging: Legal aspects and safety concerns. *Trends in Food Science & Technology, 19*(SUPPL. 1), S103–S112. https://doi.org/10.1016/J.TIFS.2008.09.011

Demarco, F., Rômio, A. P., da Trindade Alfaro, A., & Tonial, I. B. (2022). Effects of natural antioxidants on the lipid oxidation, physicochemical and sensory characteristics, and shelf life of sliced salami. *Food and Bioprocess Technology, 15*(10), 2282–2293. https://doi.org/10.1007/s11947-022-02877-2

Dilkes-Hoffman, L. S., Pratt, S., Laycock, B., Ashworth, P., & Lant, P. A. (2019). Public attitudes towards plastics. *Resources, Conservation and Recycling, 147*, 227–235. https://doi.org/10.1016/j.resconrec.2019.05.005

Dinu, M. V., Cocarta, A. I., & Dragan, E. S. (2016). Synthesis, characterization and drug release properties of 3D chitosan/clinoptilolite biocomposite cryogels. *Carbohydrate Polymers, 153*, 203–211. https://doi.org/10.1016/J.CARBPOL.2016.07.111

Dragan, E. S., & Dinu, M. V. (2020). Advances in porous chitosan-based composite hydrogels : Synthesis and applications. *Reactive and Functional Polymers*, *146*, 104372. https://doi.org/10.1016/j.reactfunctpolym.2019.104372

Duarte, L. G. R., Ferreira, N. C. A., Fiocco, A. C. T. R., & Picone, C. S. F. (2022). Lactoferrin-chitosan-TPP nanoparticles: Antibacterial action and extension of strawberry shelf-life. *Food and Bioprocess Technology*, 135–148. https://doi.org/10.1007/s11947-022-02927-9

El Miri, N., Abdelouahdi, K., Barakat, A., Zahouily, M., Fihri, A., Solhy, A., & El Achaby, M. (2015). Bio-nanocomposite films reinforced with cellulose nanocrystals: Rheology of film-forming solutions, transparency, water vapor barrier and tensile properties of films. *Carbohydrate Polymers, 129*, 156–167. https://doi.org/10.1016/J.CARBPOL.2015.04.051

Emir, A. A., Yildiz, E., Aydogdu, Y., & Sumnu, G. (2022). Active films based on Faba Bean (Vicia faba L.) flour incorporated with Sumac (Rhus coriaria): Assessment of antioxidant and antimicrobial performances of packaging for shelf life of chicken breast. *Food and Bioprocess Technology*, 327–341. https://doi.org/10.1007/s11947-022-02940-y

Fernández, A., Soriano, E., López-Carballo, G., Picouet, P., Lloret, E., Gavara, R., & Hernández-Muñoz, P. (2009). Preservation of aseptic conditions in absorbent pads by using silver nanotechnology. *Food Research International, 42*(8), 1105–1112. https://doi.org/10.1016/J.FOODRES.2009.05.009

Friedrich, D. (2020). How regulatory measures towards biobased packaging influence the strategic behaviour of the retail industry: A microempirical study. *Journal of Cleaner Production*, *260*, 121128. https://doi.org/10.1016/j.jclepro.2020.121128

Gao, P., Cha, R., Luo, H., Xu, Y., Zhang, P., Han, L., et al. (2021). Development of antimicrobial oxidized cellulose film for active food packaging. *Carbohydrate Polymers*, 118922. https://doi.org/10.1016/j.carbpol.2021.118922

Gokmen, F. O., Yaman, E., & Temel, S. (2021). Eco-friendly polyacrylic acid based porous hydrogel for heavy metal ions adsorption: Characterization, adsorption behavior, thermodynamic and reusability studies. *Microchemical Journal*, *168*, 106357. https://doi.org/10.1016/j.microc.2021.106357

Haghighi, H., Gullo, M., La China, S., Pfeifer, F., Siesler, H. W., Licciardello, F., & Pulvirenti, A. (2021). Characterization of bionanocomposite films based on gelatin/polyvinyl alcohol blend reinforced with bacterial cellulose nanowhiskers for food packaging applications. *Food Hydrocolloids*, *113*, 106454. https://doi.org/10.1016/j.foodhyd.2020.106454

Haghighi, H., Leugoue, S. K., Pfeifer, F., Siesler, H. W., Licciardello, F., Fava, P., & Pulvirenti, A. (2020). Development of antimicrobial films based on chitosan-polyvinyl alcohol blend enriched with ethyl lauroyl arginate (LAE) for food packaging applications. *Food Hydrocolloids*, *100*, 105419. https://doi.org/10.1016/j.foodhyd.2019.105419

Hebeish, A., Hashem, M., El-hady, M. M. A., & Sharaf, S. (2013). Development of CMC hydrogels loaded with silver nano-particles for medical applications. *Carbohydrate Polymers, 92*(1), 407–413. https://doi.org/10.1016/j.carbpol.2012.08.094

Huang, J., Lyu, S., Fu, F., Wu, Y., & Wang, S. (2017). Green preparation of a cellulose nanocrystals/ polyvinyl alcohol composite superhydrophobic coating. *RSC Advances, 7*(33), 20152–20159. https://doi.org/10.1039/c6ra27663f

Hui, J., Li, H., Zheng, X., Ma, H., Fan, D., Liu, H., & Wang, Y. (2015). Control synthesis and self-assembly of calcium apatite at low temperatures. *Ceramics International, 41*(5), 6194–6202. https://doi.org/10.1016/j.ceramint.2014.12.156

Jayakumar, A., K.V., H., T.S., S., Joseph, M., Mathew, S., G., P., et al. (2019). Starch-PVA composite films with zinc-oxide nanoparticles and phytochemicals as intelligent pH sensing wraps for food packaging application. *International Journal of Biological Macromolecules, 136*, 395–403. https://doi.org/10.1016/j.ijbiomac.2019.06.018

Kameshwar, A. K. S., & Qin, W. (2016). Recent developments in using advanced sequencing technologies for the genomic studies of lignin and cellulose degrading microorganisms. *International Journal of Biological Sciences, 12*(2), 156–171. https://doi.org/10.7150/ijbs.13537

Koçyiğit, S., Gökmen, Ö., Temel, S., Aytimur, A., Uslu, I., & Haman Bayari, S. (2013). Structural investigation of boron undoped and doped indium stabilized bismuth oxide nanoceramic powders. *Ceramics International, 39*(7), 7767–7772. https://doi.org/10.1016/j.ceramint.2013.03.035

Koenig-Lewis, N., Grazzini, L., & Palmer, A. (2022). Cakes in plastic: A study of implicit associations of compostable bio-based versus plastic food packaging. *Resources, Conservation and Recycling*, *178*, 105977. https://doi.org/10.1016/j.resconrec.2021.105977

Li, S., Sun, X., Li, H., & Yan, S. (2018). The crystallization behavior of biodegradable polymer in thin fi lm. *European Polymer Journal, 102*, 238–253. https://doi.org/10.1016/j.eurpolymj.2018.03.029

Liu, B., Xu, H., Zhao, H., Liu, W., Zhao, L., & Li, Y. (2017). Preparation and characterization of intelligent starch/PVA films for simultaneous colorimetric indication and antimicrobial activity for food packaging applications. *Carbohydrate Polymers, 157*, 842–849. https://doi.org/10.1016/j.carbpol.2016.10.067

Liu, J., Cheng, D., Zhang, D., Han, L., Gan, Y., Zhang, T., & Yu, Y. (2022). Incorporating ε-polylysine hydrochloride, tea polyphenols, nisin, and ascorbic acid into edible coating solutions: Effect on quality and shelf life of marinated eggs. *Food and Bioprocess Technology, 15*(12), 2683–2696. https://doi.org/10.1007/s11947-022-02908-y

Luo, Y., Su, J., Guo, S., Cao, Z., Liu, Z., Wu, S., et al. (2022). Preparation of humidity-responsive cinnamon essential oil nanomicelles and its effect on postharvest quality of strawberries. *Food and Bioprocess Technology, 15*(12), 2723–2736. https://doi.org/10.1007/s11947-022-02906-0

Ma, W., Li, L., Xiao, X., Du, H., Ren, X., Zhang, X., et al. (2020). 2000228 (1 of 9) Construction of chlorine labeled ZnO-chitosan loaded cellulose nanofibrils film with quick antibacterial performance and prominent UV stability. *Macromolecular Materials and Engineering, 305*, 2000228. https://doi.org/10.1002/mame.202000228

Mahroug, H., Mansri, A., & Dergal, F. (2019). The effect of calcium suspension concentration on the hydroxyapatite structures and purity. *Revue Roumaine de Chimie*, *64*(3), 277–286. https://doi.org/10.33224/rrch/2019.64.3.10

Mansri, A., Mahroug, H., & Dergal, F. (2019). In situ preparation of hydroxyapatite composites into hydrolyzed polyacrylamide solution and methylene blue dye retention. *Turkish Journal of Chemistry, 43*(2), 582–593. https://doi.org/10.3906/kim-1803-49

Mary, I. R., Sonia, S., Viji, S., Mangalaraj, D., Viswanathan, C., & Ponpandian, N. (2016). Novel multiform morphologies of hydroxyapatite: Synthesis and growth mechanism. *Applied Surface Science, 361*, 25–32. https://doi.org/10.1016/j.apsusc.2015.11.123

Misra, K., & S., P. Valappil, S., Roy, I., & R. Boccaccini, A. (2006). Polyhydroxyalkanoate (PHA)/inorganic phase composites for tissue engineering applications. *Biomacromolecules, 7*(8), 2249–2258. https://doi.org/10.1021/bm060317c

Min, T., Zhu, Z., Sun, X., Yuan, Z., Zha, J., & Wen, Y. (2020). Highly efficient antifogging and antibacterial food packaging film fabricated by novel quaternary ammonium chitosan composite. *Food Chemistry*, *308*, 125682. https://doi.org/10.1016/j.foodchem.2019.125682

Montheard, J. -P., Chatzopoulos, M., & Chappard, D. (1992). 2-Hydroxyethyl methacrylate (HEMA): Chemical properties and applications in biomedical fields. *Journal of Macromolecular Science, Part C, 32*(1), 1–34. https://doi.org/10.1080/15321799208018377

Muratore, F., Barbosa, S. E., & Martini, R. E. (2019). Development of bioactive paper packaging for grain-based food products. *Food Packaging and Shelf Life*, *20*, 100317. https://doi.org/10.1016/j.fpsl.2019.100317

Nair, L. S., & Laurencin, C. T. (2007). Biodegradable polymers as biomaterials. *Progress in Polymer Science, 32*(8–9), 762–798. https://doi.org/10.1016/J.PROGPOLYMSCI.2007.05.017

Nguyen, H., Hong, T., Tan, L., Jeon, H., & Oh, D. X. (2021). Biorenewable , transparent , and oxygen / moisture barrier nanocellulose / nanochitin-based coating on polypropylene for food packaging applications. *Carbohydrate Polymers*, *271*, 118421. https://doi.org/10.1016/j.carbpol.2021.118421

Otoni, C. G., Espitia, P. J. P., Avena-Bustillos, R. J., & McHugh, T. H. (2016). Trends in antimicrobial food packaging systems: Emitting sachets and absorbent pads. *Food Research International, 83*, 60–73. https://doi.org/10.1016/J.FOODRES.2016.02.018

Oyen, M. L. (2014). Mechanical characterisation of hydrogel materials. *International Materials Reviews, 59*(1), 44–59. https://doi.org/10.1179/1743280413Y.0000000022

Ozdemir, M., & Floros, J. D. (2004). Active food packaging technologies. *Critical Reviews in Food Science and Nutrition, 44*(3), 185–193. https://doi.org/10.1080/10408690490441578

Pereira, A. T., Henriques, P. C., Costa, P. C., Martins, M. C. L., Magalhães, F. D., & Gonçalves, I. C. (2019). Graphene oxide-reinforced poly(2-hydroxyethyl methacrylate) hydrogels with extreme stiffness and high-strength. *Composites Science and Technology*, *184*, 107819. https://doi.org/10.1016/j.compscitech.2019.107819

Piyada, K., Waranyou, S., & Thawien, W. (2013). Mechanical, thermal and structural properties of rice starch films reinforced with rice starch nanocrystals. *International Food Research Journal, 20*(1), 439–449.

Rooney, M. L. (2005). Introduction to active food packaging technologies. *Innovations in Food Packaging*, 63–79. https://doi.org/10.1016/B978-012311632-1/50037-1

Shahabi-Ghahfarrokhi, I., & Babaei-Ghazvini, A. (2019). Using photo-modification to compatibilize nano-ZnO in development of starch-kefiran-ZnO green nanocomposite as food packaging material. *International Journal of Biological Macromolecules, 124*, 922–930. https://doi.org/10.1016/j.ijbiomac.2018.11.241

Sumrin, S., Gupta, S., Asaad, Y., Wang, Y., Bhattacharya, S., & Foroudi, P. (2021). Eco-innovation for environment and waste prevention. *Journal of Business Research, 122*, 627–639. https://doi.org/10.1016/j.jbusres.2020.08.001

Suppakul, P., Sonneveld, K., Bigger, S. W., & Miltz, J. (2008). Efficacy of polyethylene-based antimicrobial films containing principal constituents of basil. *LWT - Food Science and Technology, 41*(5), 779–788. https://doi.org/10.1016/J.LWT.2007.06.006

Tang, Y., Hu, X., Zhang, X., Guo, D., Zhang, J., & Kong, F. (2016). Chitosan/titanium dioxide nanocomposite coatings: Rheological behavior and surface application to cellulosic paper. *Carbohydrate Polymers, 151*, 752–759. https://doi.org/10.1016/j.carbpol.2016.06.023

Temel, S., Gokmen, F. O., & Yaman, E. (2020). Antibacterial activity of ZnO nanoflowers deposited on biodegradable acrylic acid hydrogel by chemical bath deposition. *Bulletin of Materials Science, 43*(1), 1–6. https://doi.org/10.1007/s12034-019-1967-1

Temel, S., Gökmen, F., & Yaman, E. (2019a). An energy efficient way to produce zinc-based semiconductor thin films via chemical bath deposition technique. *Journal of Sustainable Development of Energy, Water and Environment Systems*, *7*(2), 253–260. https://doi.org/10.13044/j.sdewes.d6.0239

Temel, S., Yaman, E., Ozbay, N., & Gokmen, F. O. (2019b). Synthesis, characterization and adsorption studies of nano-composite hydrogels and the effect of SiO2on the capacity for the removal of Methylene Blue dye. *Journal of the Serbian Chemical Society, 85*(7), 939–952. https://doi.org/10.2298/JSC190517114T

Thompson, J. M., Waites, W. M., & Dodd, C. E. R. (1998). Detection of rope spoilage in bread caused by bacillus species. *Journal of Applied Microbiology, 85*(3), 481–486. https://doi.org/10.1046/j.1365-2672.1998.853512.x

Vélez-Erazo, E. M., Carbajal-Sandoval, M. S., Sanchez-Pizarro, A. L., Peña, F., Martínez, P., & Velezmoro, C. (2022). Peruvian biopolymers (sapote gum, tunta, and potato starches) as suitable coating material to extend the shelf life of bananas. *Food and Bioprocess Technology, 15*(11), 2562–2572. https://doi.org/10.1007/s11947-022-02902-4

Wang, F., Chen, C., Wang, J., Xu, Z., Shi, F., & Chen, N. (2023). Facile preparation of PHEMA hydrogel induced via Tannic Acid-Ferric ions for wearable strain sensing. *Colloids and Surfaces A: Physicochemical and Engineering Aspects*, *658*, 130591. https://doi.org/10.1016/j.colsurfa.2022.130591

Wang, Y., Ouyang, H., Xie, Y., Jiang, Y., Zhao, L., Peng, W., et al. (2022). Mechanically robust, biocompatible, and durable PHEMA-based hydrogels enabled by the synergic effect of strong intermolecular interaction and suppressed phase separation. *Polymer*, *254*, 125083. https://doi.org/10.1016/j.polymer.2022.125083

Wichterle, O., & Lím, D. (1960). Hydrophilic gels for biological use. *Nature, 185*(4706), 117–118. https://doi.org/10.1038/185117a0

Wu, M., Sukyai, P., Lv, D., Zhang, F., Wang, P., Liu, C., & Li, B. (2020). Water and humidity-induced shape memory cellulose nanopaper with quick response, excellent wet strength and folding resistance. *Chemical Engineering Journal*, *392*(August 2019), 123673. https://doi.org/10.1016/j.cej.2019.123673

Yang, X., Huang, L., Zhou, L., Xu, H., & Yi, Z. (2016). A photochromic copolymer hydrogel contact lens: From synthesis to application. *International Journal of Polymer Science*, *2016*(Cd). https://doi.org/10.1155/2016/4374060

Yavuz, M., Çakir, O., & Baysal, Z. (2016). Adsorption of cellulase on poly(2-hydroxyethyl methacrylate) cryogels containing phenylalanine. *Turkish Journal of Chemistry, 40*(5), 720–728. https://doi.org/10.3906/kim-1601-43

Youssef, A. M., El-Sayed, H. S., El-Sayed, S. M., Fouly, M., & El-Aziz, M. E. A. (2022). Novel bionanocomposites based on cinnamon nanoemulsion and TiO2-NPs for preserving fresh chicken breast fillets. *Food and Bioprocess Technology*, 356–367. https://doi.org/10.1007/s11947-022-02934-w

Zhang, L., Lyu, S., Zhang, Q., Wu, Y., Melcher, C., Chmely, S. C., et al. (2019). Dual-emitting film with cellulose nanocrystal-assisted carbon dots grafted SrAl2O4, Eu2+, Dy3+ phosphors for temperature sensing. *Carbohydrate Polymers, 206*, 767–777. https://doi.org/10.1016/j.carbpol.2018.11.031